

Published in final edited form as:

Nat Cell Biol. 2010 January ; 12(1): 87–18. doi:10.1038/ncb2009.

Carbonic Anhydrases are Upstream Regulators in Guard Cells of CO₂-Controlled Stomatal Movements

Honghong Hu^{1,5}, Aurélien Boisson-Dernier^{1,2,5}, Maria Israelsson-Nordström^{1,3,5}, Maik Böhmer^{1,6}, Shaowu Xue^{1,4,6}, Amber Ries¹, Jan Godoski¹, Josef M. Kuhn¹, and Julian I. Schroeder^{1,7}

¹Division of Biological Sciences, Cell and Developmental Biology Section, University of California San Diego, La Jolla, CA 92093-0116, USA.

Abstract

The continuing rise in atmospheric CO₂ causes closing of stomatal pores in leaves and thus globally affects CO₂ influx into plants, water use efficiency and leaf heat stress^{1–4}. However, the CO₂-binding proteins that control this response remain unknown. Moreover, the cell type that responds to CO₂, mesophyll or guard cells, and whether photosynthesis mediates this response are matters of debate^{5–8}. We demonstrate that *Arabidopsis* double mutant plants in the β-carbonic anhydrases, βCA1 and βCA4, display impaired CO₂-regulation of stomatal movements and increased stomatal density, but retain functional abscisic-acid and blue-light responses. βCA-mediated CO₂-triggered stomatal movements are not, in-first-order, linked to leaf-photosynthesis and can function in guard cells. Furthermore, guard cell βCA-over-expression plants exhibit enhanced water use efficiency. Guard cell-expression of mammalian *αCAII* complements *calca4* shows that carbonic anhydrase-mediated catalysis is an important mechanism for βCA-mediated CO₂-induced stomatal closing and patch clamp analyses indicate that CO₂/HCO₃[–] transfers the signal to anion channel regulation. These findings, together with *ht1-2*⁹ epistasis analysis demonstrate that carbonic anhydrases function early in the CO₂ signalling pathway that controls gas-exchange between plants and the atmosphere.

Guard cells form adjustable stomatal pores in the plant epidermis that allow CO₂ influx for photosynthesis in exchange for transpirational water loss from plants to the atmosphere. The continuing rise in atmospheric [CO₂] and the resulting increase in leaf intercellular [CO₂] (C_i) is causing a reduction in stomatal apertures across diverse plant species². To date, only a few *Arabidopsis* mutants have been characterized that show CO₂ insensitivity in stomatal movement regulation^{10–14}. However, these mutants also exhibit insensitivity to the hormone abscisic acid (ABA), consistent with present models that the encoded proteins function downstream of a convergence point of the CO₂ and ABA stomatal closure signalling pathways^{10, 12–14}. The only *Arabidopsis* protein proposed to function upstream of

⁷Correspondence should be addressed to J. I. S. (julian@biomail.ucsd.edu).

²Present address: Department of Developmental Genetics, University of Zürich, CH-8008 Zürich, Switzerland.

³Present address: Department of Botany, Stockholm University, SE-10691 Stockholm, Sweden.

⁴Permanent address: Institute of Molecular Science, Shanxi University, Taiyuan, 030006, China

⁵These authors contributed equally to this work.

⁶These authors contributed equally to this work.

AUTHOR CONTRIBUTIONS

J.I.S. conceived of the project and proposed the experimental design. H.H., A. B.-D. and M.I.-N. performed most of the experiments and contributed equally to the work. M.B. performed CA activity analyses. S. X. performed patch clamp experiments. A.R. contributed to stomatal movement and stomatal index measurements. J. G. performed norflurazon experiments. J.M.K. analyzed CO₂-HCO₃[–]-binding protein-encoding gene expression patterns and isolated the initial CA, PEPC and Rubisco T-DNA insertion lines. J.I.S., H.H., A.B.-D. and M.I.-N. wrote the paper.

this convergence point is the negative regulator of CO₂-induced stomatal closure, HIGH LEAF TEMPERATURE 1 kinase, for which mutations cause a constitutive high-[CO₂] response⁹. The ABC transporter AtABCB14 identified as a malate uptake transporter in the guard cell plasma membrane also functions as a negative regulator of high [CO₂]-induced stomatal closure¹⁵. Antisense repression of a MAP Kinase (NtMKP4) in tobacco reduces CO₂ regulation of stomatal conductance but not ABA responses¹⁶. The CO₂-/HCO₃⁻-binding proteins, Rubisco and PEP carboxylases (PEPC), have been investigated for their putative participation in high CO₂-induced stomatal closure^{5, 17, 18}. However, it was shown that CO₂-regulated stomatal conductance is independent of Rubisco activity⁵ and that PEPC levels had no direct effect on high CO₂-triggered stomatal closing^{17, 18} (see also Supplementary Results). As no CO₂-binding proteins have been identified in genetic screens of CO₂-regulated stomatal signalling, we postulated that CO₂-binding proteins that mediate this response may underlie a gene family with overlapping gene functions, similar to other stomatal movement control mechanisms^{19, 20}.

We hypothesized that the CO₂-binding proteins carbonic anhydrases that catalyze the reversible reaction of CO₂ + H₂O ⇌ HCO₃⁻ + H⁺, might function early in CO₂ signaling (see also Supplementary Results). Transcriptome analyses of mesophyll and guard cells show that the β-carbonic anhydrases *βCA1* (At3g01500), *βCA4* (At1g70410) and *βCA6* (At1g58180) are highly expressed in guard cells and/or mesophyll cells (Fig. 1a)^{21, 22} which was confirmed by quantitative RT-PCR (Fig. 1b). Consistent with these data, *βCA1* and *βCA4* were also detected in the guard cell proteome²³.

Single T-DNA disruption mutant plants in *βCA1*, *βCA4* and *βCA6* did not display strong phenotypes in CO₂ responses in mature leaves. *calca4*, *ca4ca6*, *calca6* double mutants as well as *calca4ca6* triple mutant were subsequently generated for assessment of their CO₂ sensitivities. Interestingly, *calca4* double and *calca4ca6* triple mutant plants showed strong insensitivities in CO₂-induced stomatal conductance changes (Fig. 1c–e; Supplementary Information, S1d–h). However, *calca6* and *ca4ca6* mutants did not exhibit an altered CO₂ response, indicating no major role for the more distantly-related βCA6 (Supplementary Information, Fig. S1b, c). CO₂-induced stomatal conductance changes in *calca4* were greatly impaired during ambient (365 ppm) to 800 ppm or 400 to 100 ppm [CO₂] changes at both 55 μmol m⁻²s⁻¹ and 1000 μmol m⁻²s⁻¹ light fluence rates (Fig. 1c–e; Supplementary Information, Fig. S1e–h). However, more dramatic shifts from 800 to 100 ppm and from 100 to 800 ppm [CO₂], triggered stomatal conductance changes in *calca4* plants, although at slower rates compared to wild-type plants (see captions of Fig. 1d, e). Furthermore, *calca4* plants consistently showed a higher stomatal conductance at ambient [CO₂] (365–400 ppm) compared to wild-type plants (Fig. 1d, e; Supplementary Information, Fig. S1f). Interestingly, stomatal index (SI) and stomatal density (SD) were significantly higher in *calca4* (SI: 27 ± 0.9%; SD: 188 ± 13.2 per mm²) compared to wild type (SI: 22 ± 0.6%; SD: 142.5 ± 15.4 stomata per mm², means ± s.e.m.), and this 1.3-fold increase in stomatal density could in part account for the higher stomatal conductance observed in *calca4* leaves.

In clear contrast to the impaired CO₂ responses (Fig. 1c–e), and despite the higher starting stomatal conductance of the *βca* mutant plants (Fig. 1d, e), *calca4* and *calca4ca6* plants showed robust responses to blue light and blue light to dark transitions (Fig. 1f; Supplementary Information, Fig. S2a–c). The initial rates of stomatal conductance changes triggered by blue light were not significantly different between *βca* mutants and wild type (Supplementary information, captions to Fig. S2a, b). CO₂ responses were also analyzed in leaf epidermes, which had been removed from their mesophyll cell environment. High [CO₂]-induced stomatal closure was greatly impaired in *calca4* compared to wild type after 30 min (Fig. 1g) or 60 min (Supplementary Information, Fig. S2d) exposure. Thus, the impaired CO₂ responses in intact leaves correlate with impaired CO₂-induced stomatal

movements. In sharp contrast to other known CO₂-insensitive mutants^{12–14}, ABA-induced stomatal closing remained clearly functional in *calca4* leaf epidermes (Fig. 1h), consistent with a model that β CA1 and β CA4 function early in CO₂ signal transduction.

Biochemical carbonic anhydrase activities in mature leaves of 5–7 week-old *cal*, *ca4* single mutants and *calca4* were analyzed. The *calca4* mutant plants showed a \approx 65 % reduction in CO₂ hydration reactions compared to wild type (Fig. 2a). Introduction of a genomic copy of either β CA1 or β CA4 in *calca4* restored the expression of the respective gene (Fig. 2b) and complemented the CO₂-responsive phenotype in six randomly selected transgenic lines (Fig. 2c, d; Supplementary Information, Fig. S3). Moreover, all transgenic lines showed wild-type-like stomatal densities and indices (Supplementary Information, Fig. S4). Thus, disruption of β CA1 and β CA4 is indeed responsible for the CO₂ insensitive stomatal movement regulation and the stomatal density phenotypes observed in *calca4* and expression of either gene is sufficient for complementation of both phenotypes.

β CA1 and β CA4 have been identified in chloroplasts (β CA1) and at the plasma membrane in proteome and imaging analyses^{24–26}. Consistent with these studies, β CA1-YFP and β CA4-YFP subcellular localization analyses suggest that β CA1 localizes to both chloroplasts and in the vicinity of the plasma membrane, while β CA4 localizes in the vicinity of the plasma membrane (Supplementary Information, Figs. S5, 6). As these subcellular localizations may indicate roles in transcellular carbon delivery to chloroplasts, as reported for aquaporins²⁷, we analyzed whether the role of β CAs in CO₂-induced stomatal closing is dependent on mature leaf photosynthesis. Photosynthesis was inhibited in newly emerging leaves of plants watered with the carotenoid biosynthesis inhibitor norflurazon (Fig. 3a–c). However CO₂-induced stomatal closing remained functional in chlorophyll-deficient “albino” leaves (Fig. 3d), as previously reported in *Vicia faba*⁷. More direct genetic analyses in *calca4ca6* mutant plants showed no differences to wild-type plants in the maximum efficiency of photosystem II (F_v/F_m) (Fig. 3e, $n = 10$), or the quantum yield of photosystem II (Φ_{PSII}) at low (50 $\mu\text{mol m}^{-2}\text{s}^{-1}$, $n = 6$) and high (2000 $\mu\text{mol m}^{-2}\text{s}^{-1}$, $n = 6$) light conditions (Fig. 3f, g). CO₂ assimilation rates of *calca4ca6* plants in response to darkness to 300 $\mu\text{mol m}^{-2}\text{s}^{-1}$ red light shifts were also unaffected (Fig. 3h). Therefore, the stomatal CO₂ response in *Arabidopsis* proceeds in the absence of chlorophyll (Fig. 3a–d) and mature leaf photosynthetic activities are not impaired in *calca4ca6* under the imposed growth conditions (Fig. 3e–h). Note that other growth conditions and other *ca* mutant combinations may lead to effects of CAs on photosynthetic activities, given the chloroplast location of β CA1 and proposed roles of CAs in photosynthetic activities.

To analyze whether β CA expression targeted to guard cells is sufficient to complement the CO₂ insensitive phenotype of *calca4*, β CA1 or β CA4 cDNA driven by a strong guard cell promoter *pGCI*²² was transformed into *calca4*. In these stably transformed *calca4* lines, β CA1 and β CA4 transcripts were detected in guard cells but not in mesophyll cells (Fig. 4a; Supplementary Information, Fig. S7a). Four randomly selected independent transgenic lines expressing β CA1 or β CA4 in guard cells exhibited recovery of CO₂ responsiveness (Fig. 4b; Supplementary Information, Fig. S7b–d). Interestingly, in contrast to *calca4*, these transgenic lines displayed wild-type-like stomatal indices and densities (Supplementary Information, Fig. S7e, f). Thus, targeted expression of β CA1 or β CA4 in guard cells is sufficient to restore CO₂ responsiveness and stomatal density.

We then investigated whether over-expression of β CA1 or β CA4 in guard cells of wild-type plants can modulate intact plant gas exchange. Four randomly selected independent lines over-expressing β CA1 or β CA4 in the wild-type background (Supplementary Information, Fig. S8b) displayed a reduced stomatal conductance at all tested [CO₂] (Fig. 4c; Supplementary Information, Fig. S8c–e). Interestingly, substantial increases in the

instantaneous water use efficiency (WUE) of all analyzed guard cell-targeted over-expression lines were consistently found, with an average increase of 44% at ambient $[\text{CO}_2]$ (Fig. 4d), while CO_2 assimilation rates were not significantly altered under the imposed growth conditions (Fig. 4e). All over-expressing lines exhibited reduced fresh weight loss from excised leaves compared to wild type (Supplementary Information, Fig. S8f), consistent with a reduced stomatal conductance at ambient $[\text{CO}_2]$ in all βCA -overexpressing lines (Fig. 4c; Supplementary Information, Fig. S8c–e).

No whole plant phenotypic growth differences and no reduction in total plant dry weight (growth penalty) were observed in βCA -overexpressing lines compared to wild-type plants under limited-watering or well-watered conditions (Supplementary Information, Fig. S8a, g, h). Guard cell-targeted overexpression lines displayed slightly lower average stomatal densities (–13%) and stomatal indices (–14%) compared to parallel grown wild-type plants (Supplementary Information, Fig. S9; $P = 0.0312$ to 0.0523 for these overexpression lines compared to wild type, Student's t -test). The “single cell spacing phenotype” was not violated in *calca4* mutant and βCA -overexpression plants leaves^{28, 29}. Therefore, guard cell-targeted over-expression of βCA is sufficient to modulate CO_2 regulation of stomatal conductance and may provide an approach for improving the water use efficiency of C3 plants.

The earliest component of CO_2 signalling in *Arabidopsis* guard cells identified thus far is the HT1 protein kinase, a negative regulator of the CO_2 response pathway⁹. The recessive *ht1-2* allele exhibits a constitutive high- $[\text{CO}_2]$ response⁹. Strikingly, *calca4ht1-2* triple mutant plants exhibited a constitutive high- $[\text{CO}_2]$ phenotype similar to *ht1-2* (Fig. 5a), showing that HT1 is epistatic to βCA1 and βCA4 and supporting an early CO_2 signalling role of βCAs . To determine whether enzymatic carbonic anhydrase activity mediates CO_2 control of gas exchange, we expressed an unrelated α -carbonic anhydrase from human, αCAII ³⁰, under the control of the guard cell promoter in *calca4* plants. Human αCAII shows only 9% identity to βCA1 and 12% to βCA4 at the amino acid level, respectively. Astonishingly, three randomly-selected independent human αCAII -expressing transgenic *calca4* lines (Fig. 5b) exhibited restoration of the CO_2 insensitive phenotype, providing strong evidence that carbonic anhydrase activity in guard cells is required for CO_2 -mediated stomatal regulation (Fig. 5c; Supplementary Information, Fig. S10).

To determine whether the carbonic anhydrase reaction product, intracellular bicarbonate, can participate in stomatal signalling, S-type anion channel regulation was analyzed. Addition of 6.75 mM bicarbonate and buffering free $[\text{CO}_2]$ to 1 mM at pH 7.1 resulted in typical small background currents (Fig. 5d, $n = 6$). In contrast, when 13.5 mM bicarbonate was added, which buffered free $[\text{CO}_2]$ to 2 mM at pH 7.1, strong S-type anion currents were observed in guard cells, demonstrating that plasma-membrane anion channels can be activated by $\text{CO}_2/\text{HCO}_3^-$, though at high concentrations (Fig. 5d, $n = 10$). Furthermore, extracellularly applied bicarbonate buffered to 2 mM free $[\text{CO}_2]$ in the bath solution caused a smaller activation of S-type anion currents in guard cells compared to that of intracellular bicarbonate ($P < 0.01$ at -147mV and -117mV , pairwise Student's t -test, Supplementary Information, Fig. S10c). These data indicate that HCO_3^- emanating from neighboring cells may be taken up by guard cells and might contribute to the stomatal response, albeit at a lower level. These results demonstrate for the first time that elevated intracellular bicarbonate and CO_2 levels can contribute to activation of guard cell plasma-membrane anion channel currents and indicate that $\text{CO}_2/\text{HCO}_3^-$ flux may function in βCA -mediated CO_2 -induced stomatal closing.

The present data show that β -carbonic anhydroses function very early in the CO_2 -induced stomatal signal transduction cascade based on impaired CO_2 responses yet robust responses

to blue light, light-dark transitions and abscisic acid in *calca4* leaves and epistasis analyses with the *ht1-2* mutant⁹. The differential CO₂ response of wild-type and *calca4* in isolated leaf epidermes, together with guard cell-targeted complementation of *calca4* by β CA and even by the unrelated human α CAII as well as guard cell β CA over-expression plant phenotypes provide genetic and molecular evidence that guard cells are a major site for β -carbonic anhydrase-mediated CO₂ regulation of stomatal movements. However, the existence of an additional mesophyll- and/or a photosynthesis-related pathway^{6, 8} contributing to the residual CO₂-induced stomatal movements in *calca4* (Fig. 1c-e) cannot be strictly excluded. The residual and slowed CO₂ responses in *beta* mutant leaves may result from a combination of: (a) additional carbonic anhydrases that are expressed in guard cells^{21, 22}; (b) CO₂ levels may be elevated in *calca4* guard cells compared to wild type, due to the reduced CO₂ hydration activity found in *calca4*; (c) non-guard cell tissues such as pavement cells and mesophyll cells may contribute to the residual CO₂ response; (d) a parallel mechanism for CO₂ signalling and (e) even in the absence of carbonic anhydrases a slow spontaneous reversible hydration of CO₂ occurs.

Interestingly, an increased stomatal density in *calca4* and an opposite effect in β CA guard cell-overexpression plants were observed, indicating that β CA1/4 not only strongly affect CO₂ control of stomatal movements but also modulate stomatal development at ambient [CO₂]. Analyses of the *pGCI* guard cell promoter activity during stomatal development²² further suggest that β CA-mediated control of stomatal development is non cell-autonomous, as stomatal development is defined prior to the guard cell stage^{28, 29}. Previous studies have suggested non cell-autonomous long distance signalling from mature leaves to newly developing leaves as part of the mechanisms by which environmental cues regulate stomatal development³¹. Further research is needed to determine whether β CA1 and β CA4 function in environmental control of stomatal development.

Guard cell-targeted over-expression of β CA1 or β CA4 consistently increased instantaneous water use efficiency, indicating that: (i) β CA expression levels are not saturated in wild-type guard cells; and (ii) manipulation of carbonic anhydrases may provide an approach for engineering gas exchange and transpirational water loss or alternatively protection against heat-induced damage of plants in light of the continuing atmospheric [CO₂] increase, climate change and limited global freshwater availability^{4, 32}.

Restoration of CO₂ regulation of stomatal movements by guard cell expression of the structurally unrelated human α CAII provides strong evidence that catalytic CA activity and bicarbonate and/or proton production function in mediation of this CO₂ response and indicates that CO₂ regulation of stomatal conductance in plants underlies flux control³³. A previous study has suggested that the CO₂ response is not mediated through changes in cytosolic pH³⁴. Moreover, the activation of large S-type anion channel currents by high intracellular bicarbonate levels provides evidence that CO₂/HCO₃⁻ may act as messengers contributing to guard cell CO₂ signal transduction. Note that although these CO₂/HCO₃⁻ are much higher than CO₂ concentrations used in gas exchange experiments, high CO₂ concentrations have been used in other electrophysiological studies (e. g. 30) and whole-cell dialysis during patch clamping may reduce the CO₂/HCO₃⁻ sensitivity of downstream signaling mechanisms. Together our findings reveal an essential function of guard cell-expressed carbonic anhydrases in CO₂ regulation of plant water transpiration and CO₂ influx and are consistent with a model in which β CA1 and β CA4 function in the early CO₂ response machinery in guard cells.

METHODS

Plant growth conditions and mutant genotyping

All *Arabidopsis thaliana* plants used in this study were of the *Columbia* ecotype (Col 0). Wild-type, *ht1-2* and *carbonic anhydrase* mutant plants were grown in a Conviron growth chamber (Winnipeg, Canada) (20°C, 60 to 80% humidity with a 16-h-light/8-h-dark photoperiod regime at $\sim 75 \mu\text{mol m}^{-2}\text{s}^{-1}$). The β -*carbonic anhydrase* T-DNA insertional mutants *ca1* (SALK_106570; insertion in Exon IX at nucleotide +2631), *ca4* (WiscDsLox508D11; insertion in Intron II at nucleotide +618) and *ca6* (SALK_044658; insertion in Exon V at nucleotide +691) were obtained from The *Arabidopsis* Biological Resource Center (ABRC). Genotyping PCR reactions were performed using the primer pairs CA1F-RT/CA1R-RT and CA1R-RT/LBa1 for *ca1*; CA4F-RT/CA4R-RT, and CA4R-RT/LB-Wisc for *ca4* and finally CA6F-RT/CA6R-RT and CA6F-RT/LBa1 for *ca6* (Supplementary Table 1). To confirm the *ht1-2* point mutation, the primers HT1-F and HT1-R were used to amplify a 300bp PCR fragment from plant genomic DNA which was then sequenced.

Time-resolved intact leaf stomatal conductance experiments with [CO₂] shifts

Stomatal conductance recordings from intact, mature non senescent leaves of 5 to 7 week-old plants were conducted starting 1 to 2 hrs after growth chamber light onset during mornings using a Li-6400 infrared (IRGA)-based gas exchange analyzer system with a fluorometer chamber (Li-Cor Inc., Lincoln, NE). Temperature and relative humidity were held at 20°C and approximately 60% to 70% respectively, while photon flux density was $55 \mu\text{mol m}^{-2}\text{s}^{-1}$ except for high light experiments (Supplementary Information, Fig. S1e, f) where temperature was 22°C and photon flux density was $1000 \mu\text{mol m}^{-2}\text{s}^{-1}$. Analyzed leaves always covered the whole surface of the gas exchange analyzer chamber so that all measurements would be dependent on the stomatal density and the stomatal aperture responses in the chamber.

For stomatal closing experiments, stomatal conductance was stabilized at ambient [CO₂] (365 ppm) for 30 min then [CO₂] was shifted to 800 ppm for 30 min or 60 min then changed to 100 ppm for at least 30 min. For additional experiments, stomatal conductance was stabilized at 400 ppm [CO₂] for 30 min, then [CO₂] was shifted to 100 ppm for 30 min and then changed to 800 ppm. The data presented are means of at least 3 leaves per genotype per treatment \pm s.e.m. Relative stomatal conductance values were determined by normalization relative to the last data point prior to the 365 to 800 ppm [CO₂], 400 to 100 ppm [CO₂] transitions or the dark to blue light transitions.

Instantaneous water use efficiency (WUE) defined as the ratio of CO₂ assimilated to water lost during transpiration ($\mu\text{mol CO}_2 \text{mmol}^{-1} \text{H}_2\text{O}^{-1}$) was calculated from data collected with the Li-6400 gas exchange analyzer at ambient [CO₂]. Three time points (first, medium and last point under ambient conditions) were chosen for each leaf. P values were calculated using Students *t*-test using two-tailed distribution and two-sample equal variance.

To calculate the initial rate of stomatal conductance changes in response to [CO₂] shifts ($n = 7$; Fig. 1d) or dark/blue light transitions ($n = 4$, Fig. S2a; $n = 5$, Fig. S2b) in wild-type and *calca4* or *calca4ca6* plants, Li-6400 data collected during the first 20 minutes following [CO₂] or blue light shifts were plotted and regression analyses were performed. These data are the average of the slopes of 4, 5 and 7 fits \pm s.e.m.. P values were calculated using unpaired *t*-test with two-tailed distribution and two-sample equal variance. Note that in the *calca4ca6* triple mutant an additional later slow rate of stomatal conductance increase was observed (Fig. S2b), whereas in the *calca4* mutant, normalized data show similar rates in wild-type and mutant plants (Fig. 1f, Fig. S2a).

Stomatal measurements

For responses to buffers pre-equilibrated with high CO₂ (800 ppm) in balance with air or control ambient air, intact submerged leaf epidermal layers were prepared with intact guard cells and leaf pavement cells¹². Stomatal apertures were analyzed only in stomatal complexes with no mesophyll cells in their vicinity. Leaf epidermal layers were pre-incubated for 1.5 h in pre-incubation buffer (10 mM MES, 10 mM KCl, 50 μM CaCl₂, pH 6.15) and exposed continuously to the indicated CO₂ conditions for 30 min or 60 min as described previously¹². As leaf epidermes were submerged in a solution volume of 7 ml, the likelihood of diffusible signals emanating from distant cells was remote. Fig. 1g and Fig. S2d correspond to 30 and 60 min CO₂ exposure times respectively at pH 6.15. For responses to ABA, epidermal layer were incubated in stomatal opening buffer (5 mM MES, 10 mM KCl, 50 μM CaCl₂, pH 6.15) for 3 h and exposed to the indicated ABA concentrations for 60 min. Thereafter stomatal apertures were measured. Data shown in Fig. 1g and Fig. S2d were genotype blind analyses and in Fig. 1h were genotype and [ABA] blind analyses ($n = 3$ experiments, 30 stomata per experiment and condition). For stomatal index and density analyses, 16 leaves for each genotype were analyzed per experiment from 4–5 week-old plants of similar plant sizes grown in an AR-22L *Arabidopsis* growth chamber (Percival, Iowa, 21°C, ~75% relative humidity, 320–340 ppm CO₂, 16-h-light/8-h-dark photoperiod regime at ~120 μmol m⁻² s⁻¹) and two areas (0.039mm²) in the middle region of abaxial epidermes of each leaf were measured. Stomatal index was defined as 100% * number of stomata / (number of stomata + number of epidermal cells) in each area.

Genomic and guard cell-targeted complementation of *ca1ca4*

For genomic complementation, the 4.5 Kb *βCA1* (including 2077 bp-long 5' region upstream of the start codon) and 4.3 Kb *βCA4* (including 1677 bp-long 5' region upstream of the start codon) genomic DNA fragments containing the *βCA1* and *βCA4* genes with their flanking sequences were PCR-amplified from the BACs F4P13 (accession number AC009325) and F17O7 (AC003671) and were recombined into the binary Gateway vector pHGY (RIKEN Plant Science Center, Japan) by LR reaction (Invitrogen). For guard cell-targeted expression of *βCA1* and *βCA4* cDNAs in wild type and *ca1ca4*, *βCA1* and *βCA4* full length cDNAs were amplified and recombined into the binary vector derived from pXCSG-Strep³⁵, where the 35S promoter was replaced by the guard cell-targeted promoter *pGCI*²². For human *αCAII* cDNA expression in guard cells of *ca1ca4* plants, the full-length cDNA was amplified from the cDNA clone (SC107902) which was purchased from the OriGENE (Rockville, MD) with primer pairs HmCAIIF/HmCAIIR and subcloned into the modified binary vector pGreenII0179 with the *pGCI* promoter.

RT-PCR and qRT-PCR analyses

Protoplasts of guard cells and mesophyll cells from wild-type and complementation plant leaves were isolated as described previously²¹ and total RNA samples from protoplasts and leaves were isolated as described³⁶. RT-PCR shown in Fig. 4a, 5b; and Fig. S1a, S8b were carried out for 30 cycles to amplify target sequences *βCA1* (CA1F/CA1R), *βCA4* (CA4F/CA4R), *βCA6* (CA6F/CA6R) and human *αCAII* (NM_000067) (HmCAIIF/HmCAIIR). For Fig. 2b, RT-PCR experiments were carried out for 29 cycles with the primer pairs CA1F-RT/CA1R-RT and CA4F-RT/CA4R-RT to amplify *βCA1* and *βCA4* respectively. For quantitative real-time PCR (qRT-PCR), the cDNAs obtained as above were diluted five times. Then, qRT-PCR was performed by using a LightCycler (Roche) with the SYBR Green I detection system, under the following conditions: 95°C for 10 min; 45 cycles of 95°C for 5 s, 55°C for 5 s, and 72°C for 13 s; followed by melting curve analysis. *EF-1α* (At5g60390) was selected as the reference gene according to³⁷. The primers for the six *βCAs* genes as well as *GCI* were designed according to³⁸ and are shown in Supplemental Table 1. PCR mixture at a final volume of 10 μL contained 2 μL of cDNA, 0.5 μM of each

primer, 4 mM Mg²⁺, and 1 μL of LightCycler-FastStart DNA Master SYBR Green I mixture (Roche). Quantitative data analyses were performed with the LightCycler software 4.0 (Roche).

Water loss measurements

For water-loss measurements, the weight of detached leaves, incubated abaxial side up under laboratory conditions was measured at the illustrated time points. Water loss was calculated as the percentage of initial fresh weight. For whole plant dry weight analyses, germinated plants were transferred to soil, 5 plants per pot (8.5×8.5×8.5 cm³). The soil filled in each pot before planting was the same and adjusted by weighing. Plants were grown in a growth room with 16-h-light/8-h-dark; the same amounts of water were applied to each pot. For limited watering 5 ml water was added every 2 days to each pot. For well-watered plants 8 ml water was added every day to each pot. Four-week old plants were carefully removed from the soil and washed, dried at 37°C for 5 days and dry weights were measured. Plant genotypes were blinded to the experimenter.

Carbonic anhydrase activity analyses

0.5g of mature leaf samples from 5–7 week-old and non-senescent *Arabidopsis* plants were ground in liquid nitrogen and immediately resuspended in 1 mL of extraction buffer (100 mM N, N-Bis 2-hydroxymethyl Gly)-NaOH buffer (pH 8.5), 20mM MgCl₂, 1mM EDTA). The lysate was cleared by centrifugation at 18,400 g for 10 min at 4°C. CA activity was measured by the potentiometric method³⁹ with some modifications. 50 μL of cell suspension was added to 3 mL of 20 mM Tris-Sulfate buffer (pH 8.3) in a scintillation vial maintained at 2°C. Addition of 2 mL of ice-cold CO₂-saturated water initiated the reaction and the time required for the pH change from 8.3 to 6.3 was measured.

Norflurazon-treated plants and analyses

Three to four week-old plants were watered once with a solution of ~67 μM norflurazon which was fully absorbed into the plant soil system followed by normal watering. Newly formed leaves showed chlorosis (bleaching) after one week. Norflurazon slowed the growth of plants; therefore control plants used in experiments were 4–5 weeks old, but at the same developmental stage as 6–7 week-old albino plants. Intact epidermal layers of control and norflurazon-treated albino leaves were analyzed using confocal imaging, with an excitation wavelength of 488 nm to measure chlorophyll fluorescence. The fluorescence intensity was quantified (Fig. 3c) following background subtraction using ImageJ (freeware National Institutes of Health, MD).

Photosynthetic activity measurements

Chlorophyll fluorescence (F) was measured using the fluorometer chamber of the Li-6400 system (LI-COR Inc, Lincoln, NE) with default settings. The F_v/F_m of pre-darkened leaves (6 weeks old) was calculated as $(F_m - F_0)/F_m$ ⁴⁰ ($n = 10$). The photochemical efficiency of photosynthesis (Φ_{PSII}) was determined by measuring steady-state fluorescence (F_s) and maximum fluorescence during a light saturating pulse (F'_m)⁴⁰ on fully expanded attached leaves ($n = 6$). The leaves were adapted to low ($50 \mu\text{mol m}^{-2} \text{s}^{-1}$) or high ($2000 \mu\text{mol m}^{-2} \text{s}^{-1}$) illumination consisting of 90% red light (630 nm) and 10% blue light (470 nm). In addition, the onset of photosynthetic activity was measured as CO₂ assimilation rate ($\mu\text{mol m}^{-2} \text{s}^{-1}$) in pre-darkened leaves exposed to red light. Leaves were pre-darkened until they showed stable stomatal conductance levels for a period of 30 minutes and then exposed to $300 \mu\text{mol m}^{-2} \text{s}^{-1}$ red light for 2 hrs ($n = 6$, 5–7 weeks old). Data presented as mean \pm s.e.m..

Patch clamp analyses

Arabidopsis guard cell protoplasts were isolated from rosette leaves of 4 to 6 week-old plants using a protoplast isolation solution containing 1.0% Cellulase R10, 0.5% Macerozyme R10 (Yakutt Horisha Co. Ltd, <http://www.yakutt.co.jp/yipi/en/product.html>), 0.5% bovine serum albumin, 0.1% kanamycin, 10 mM ascorbic acid, 0.1 mM KCl, 0.1 mM CaCl₂ and 500 mM D-mannitol (buffered to pH 5.5 using KOH). Whole-cell patch-clamp experiments were performed as described previously⁴¹. For analyses of S-type anion currents, the pipette solution contained 150 mM CsCl, 2 mM MgCl₂, 6.7 mM EGTA, 5 mM Mg-ATP, 5 mM Tris-GTP, 1 mM HEPES/Tris pH 7.1, and CaCl₂ was added to 2 μM free Ca²⁺. In analyses of intracellular bicarbonate/CO₂ activation of S-type anion currents, bicarbonate was freshly added to the pipette solution and the pH was adjusted to the indicated value with Tris-HCl. The addition of 13.5 mM bicarbonate buffered to 2 mM free CO₂ and 6.75 mM bicarbonate buffered to 1 mM free CO₂ in the pipette solution are calculated at pH 7.1 according to^{42, 43}. The bath solution contained 30 mM CsCl, 2 mM MgCl₂, 5 mM CaCl₂ and 10 mM Mes/Tris pH 5.6. In analyses of S-type anion channels activated by extracellular bicarbonate/CO₂, the addition of 2.4 mM bicarbonate buffered to 2 mM free CO₂ and 1.2 mM bicarbonate buffered to 1 mM free CO₂ were added to the bath solution at pH 5.6 adjusted with Tris-HCl. Before patch clamping, the guard cells were incubated in CsHCO₃-containing solution for 30–90 min. The bath solution contained 30 mM CsCl, 2 mM MgCl₂, 5 mM CaCl₂, Osmo 500 mmol/kg and 10 mM MES/Tris pH 5.6 and the pipette solution contained 150 mM CsCl, 2 mM MgCl₂, 6.7 mM EGTA, 5 mM Mg-ATP, 5 mM Tris-GTP, 6.03 CaCl₂ (2 μM free Ca²⁺), 1 mM HEPES-Tris and Osmo 500 mmol/kg, pH 7.1.

Subcellular localization of βCA-YFP protein

To generate the βCA1-YFP and βCA4-YFP constructs, 1061 bp βCA1 and 836 bp βCA4 cDNAs were amplified with the primer pairs CA1F/CA1YFPR and CA4F/CA4YFPR respectively and cloned into the binary pXCSG-YFP44. The pXCSG-YFP vector containing the plasma membrane targeted FLS2-YFP fusion was used as a positive control for membrane localization and provided by Dr. Silke Robatzek (Max Planck Institute for Plant Breeding Research, Cologne) (Robatzek et al., 2006). The pH35YG vector⁴⁵ containing the 35S-YFP was used as a positive control for cytosol and nuclear localizations. Protoplasts were prepared from infiltrated leaves as described⁴⁶. Protoplasts were stained with 2 μM FM4-64 dye for 5 min to only stain the plasma membrane. Fluorescence imaging was acquired by spinning-disc confocal microscopy. Images were captured with an electron multiplying charge-coupled device (EMCCD) camera (Cascade II: 512, Photometrics, Tucson, AZ, USA) using Metamorph software (Universal Imaging, Downington, PA, USA).

Supplementary Material

Refer to Web version on PubMed Central for supplementary material.

Acknowledgments

We thank Mohammad Maktabi, Jared Young and Cawas Engineer for preliminary analyses of *βca* mutants and Roger Xu for assistance. We thank Sam Zeeman (ETH Zürich) for suggestions and Koh Iba (Kyushu University) for providing *ht1-2* seeds. This research was supported by NSF (MCB0918220), NIH (GM060396) and in part DOE (DE-FG02-03ER15449) grants (to J.I.S.) and by fellowships from the Swedish Research Council Formas (to M. I.-N.), the Deutsche Forschungsgemeinschaft (to M. B.), EMBO (to J. M. K.) and in part from the King Abdullah University of Science and Technology (KAUST) (No. KUS-F1-021-31 to H. H.).

REFERENCES

1. Sellers PJ, et al. Modeling the exchanges of energy, water, and carbon between continents and the atmosphere. *Science* 1997;275:502–509. [PubMed: 8999789]
2. Medlyn BE, et al. Stomatal conductance of forest species after long-term exposure to elevated CO₂ concentration: a synthesis. *New Phytol* 2001;149:247–264.
3. LaDeau SL, Clark JS. Rising CO₂ levels and the fecundity of forest trees. *Science* 2001;292:95–98. [PubMed: 11292871]
4. Battisti DS, Naylor RL. Historical warnings of future food insecurity with unprecedented seasonal heat. *Science* 2009;323:240–244. [PubMed: 19131626]
5. von Caemmerer S, et al. Stomatal conductance does not correlate with photosynthetic capacity in transgenic tobacco with reduced amounts of Rubisco. *J. Exp. Bot* 2004;55:1157–1166. [PubMed: 15107451]
6. Messinger SM, Buckley TN, Mott KA. Evidence for involvement of photosynthetic processes in the stomatal response to CO₂. *Plant Physiol* 2006;140:771–778. [PubMed: 16407445]
7. Roelfsema MR, et al. Guard cells in albino leaf patches do not respond to photosynthetically active radiation, but are sensitive to blue light, CO₂ and abscisic acid. *Plant Cell Environ* 2006;29:1595–1605. [PubMed: 16898020]
8. Mott KA, Sibbersen ED, Shope JC. The role of the mesophyll in stomatal responses to light and CO₂. *Plant Cell Environ* 2008;31:1299–1306. [PubMed: 18541006]
9. Hashimoto M, et al. *Arabidopsis* HT1 kinase controls stomatal movements in response to CO₂. *Nat. Cell Biol* 2006;8:391–397. [PubMed: 16518390]
10. Webb AA, Hetherington AM. Convergence of the abscisic acid, CO₂, and extracellular calcium signal transduction pathways in stomatal guard cells. *Plant Physiol* 1997;114:1557–1560. [PubMed: 9276963]
11. Leymarie J, Vavasseur A, Lasceve G. CO₂ sensing in stomata of *abi1-1* and *abi2-1* mutants of *Arabidopsis thaliana*. *Plant Physiol. Biochem* 1998;36:539–543.
12. Young JJ, et al. CO₂ signaling in guard cells: calcium sensitivity response modulation, a Ca²⁺-independent phase, and CO₂ insensitivity of the *gca2* mutant. *Proc. Natl. Acad. Sci. USA* 2006;103:7506–7511. [PubMed: 16651523]
13. Vahisalu T, et al. SLAC1 is required for plant guard cell S-type anion channel function in stomatal signalling. *Nature* 2008;452:487–491. [PubMed: 18305484]
14. Negi J, et al. CO₂ regulator SLAC1 and its homologues are essential for anion homeostasis in plant cells. *Nature* 2008;452:483–486. [PubMed: 18305482]
15. Lee M, et al. The ABC transporter AtABCB14 is a malate importer and modulates stomatal response to CO₂. *Nat. Cell Biol* 2008;10:1217–1223. [PubMed: 18776898]
16. Marten H, et al. Silencing of NtMPK4 impairs CO₂-induced stomatal closure, activation of anion channels and cytosolic Ca²⁺ signals in *Nicotiana tabacum* guard cells. *Plant J* 2008;55:698–708. [PubMed: 18452588]
17. Gehlen J, et al. Effects of altered phosphoenolpyruvate carboxylase activities on transgenic C3 plant *Solanum tuberosum*. *Plant Mol. Biol* 1996;32:831–848. [PubMed: 8980535]
18. Cousins AB, et al. The role of phosphoenolpyruvate carboxylase during C4 photosynthetic isotope exchange and stomatal conductance. *Plant Physiol* 2007;145:1006–1017. [PubMed: 17827274]
19. Kinoshita T, et al. PHOT1 and PHOT2 mediate blue light regulation of stomatal opening. *Nature* 2001;414:656–660. [PubMed: 11740564]
20. Mori IC, et al. CDPKs CPK6 and CPK3 function in ABA regulation of guard cell S-type anion- and Ca²⁺-permeable channels and stomatal closure. *PLoS Biol* 2006;4:1749–1762.
21. Leonhardt N, et al. Microarray expression analyses of *Arabidopsis* guard cells and isolation of a recessive abscisic acid hypersensitive protein phosphatase 2C mutant. *Plant Cell* 2004;16:596–615. [PubMed: 14973164]
22. Yang Y, Costa A, Leonhardt N, Siegel RS, Schroeder JI. Isolation of a strong *Arabidopsis* guard cell promoter and its potential role as a research tool. *Pl. Methods* 2008;4:1–15.

23. Zhao Z, Zhang W, Stanley BA, Assmann SM. Functional proteomics of *Arabidopsis thaliana* guard cells uncovers new stomatal signaling pathways. *Plant Cell* 2008;20:3210–3226. [PubMed: 19114538]
24. Fabre N, Reiter IM, Becuwe-Linka N, Genty B, Rumeau D. Characterization and expression analysis of genes encoding *alpha* and *beta* carbonic anhydrases in *Arabidopsis*. *Plant Cell Environ* 2007;30:617–629. [PubMed: 17407539]
25. Kawamura Y, Uemura M. Mass spectrometric approach for identifying putative plasma membrane proteins of *Arabidopsis* leaves associated with cold acclimation. *Plant J* 2003;36:141–154. [PubMed: 14535880]
26. Froehlich JE, et al. Proteomic study of the *Arabidopsis thaliana* chloroplastic envelope membrane utilizing alternatives to traditional two-dimensional electrophoresis. *J. Proteome Res* 2003;2:413–425. [PubMed: 12938931]
27. Uehlein N, et al. Function of *Nicotiana tabacum* aquaporins as chloroplast gas pores challenges the concept of membrane CO₂ permeability. *Plant Cell* 2008;20:648–657. [PubMed: 18349152]
28. Bergmann DC, Sack FD. Stomatal development. *Annu. Rev. Plant Biol* 2007;58:163–181. [PubMed: 17201685]
29. Shpak ED, McAbee JM, Pillitteri LJ, Torii KU. Stomatal patterning and differentiation by synergistic interactions of receptor kinases. *Science* 2005;309:290–293. [PubMed: 16002616]
30. Lu J, et al. Effect of human carbonic anhydrase II on the activity of the human electrogenic Na⁺/HCO₃⁻ cotransporter NBCe1-A in *Xenopus oocytes*. *J. Biol. Chem* 2006;281:19241–19250. [PubMed: 16687407]
31. Lake JA, Quick WP, Beerling DJ, Woodward FI. Plant development. Signals from mature to new leaves. *Nature* 2001;411:154. [PubMed: 11346781]
32. Jacob EJ. Water: under pressure. *Nature* 2008;452:269. [PubMed: 18354450]
33. Price ND, Reed JL, Palsson BO. Genome-scale models of microbial cells: evaluating the consequences of constraints. *Nat. Rev. Microbiol* 2004;2:886–897. [PubMed: 15494745]
34. Brearley J, Venis MA, Blatt MR. The effect of elevated CO₂ concentrations on K⁺ and anion channels of *Vicia faba* L. guard cells. *Planta* 1997;203:145–154.
35. Witte CP, Noel LD, Gielbert J, Parker JE, Romeis T. Rapid one-step protein purification from plant material using the eight-amino acid StrepII epitope. *Plant Mol. Biol* 2004;55:135–147. [PubMed: 15604670]
36. Boisson-Dernier A, Frietsch S, Kim TH, Dizon MB, Schroeder JI. The peroxin loss-of-function mutation abstinence by mutual consent disrupts male-female gametophyte recognition. *Curr. Biol* 2008;18:63–68. [PubMed: 18160292]
37. Czechowski T, Stitt M, Altmann T, Udvardi MK, Scheible WR. Genome-wide identification and testing of superior reference genes for transcript normalization in *Arabidopsis*. *Plant Physiol* 2005;139:5–17. [PubMed: 16166256]
38. Udvardi MK, Czechowski T, Scheible WR. Eleven golden rules of quantitative RT-PCR. *Plant Cell* 2008;20:1736–1737. [PubMed: 18664613]
39. Wilbur KM, Anderson NG. Electrometric and colorimetric determination of carbonic anhydrase. *J. Biol. Chem* 1948;11
40. Genty B, Briantais JM, Baker NR. The relationship between the quantum yield of photosynthetic electron-transport and quenching of chlorophyll fluorescence. *Biochem. Biophys. Acta* 1989;990:87–92.
41. Allen GJ, Murata Y, Chu SP, Nafisi M, Schroeder JI. Hypersensitivity of abscisic acid-induced cytosolic calcium increases in the *Arabidopsis* farnesyltransferase mutant *eral-2*. *Plant Cell* 2002;14:1649–1662. [PubMed: 12119381]
42. Natelson S, Nobel D. More on blood bicarbonate measurement. *Clinical Chem* 1978;24:1082–1083. [PubMed: 657464]
43. Pigott JD. Coupled ion-selective electrode measurement of aqueous carbonate and bicarbonate ion activities. *Anal. Chem* 1989;61:638–640.
44. Feys BJ, et al. *Arabidopsis* senescence-associated gene101 stabilizes and signals within an enhanced disease susceptibility1 complex in plant innate immunity. *Plant Cell* 2005;17:2601–2613. [PubMed: 16040633]

45. Kubo M, et al. Transcription switches for protoxylem and metaxylem vessel formation. *Genes Dev* 2005;19:1855–1860. [PubMed: 16103214]
46. Walter M, et al. Visualization of protein interactions in living plant cells using bimolecular fluorescence complementation. *Plant J* 2004;40:428–438. [PubMed: 15469500]

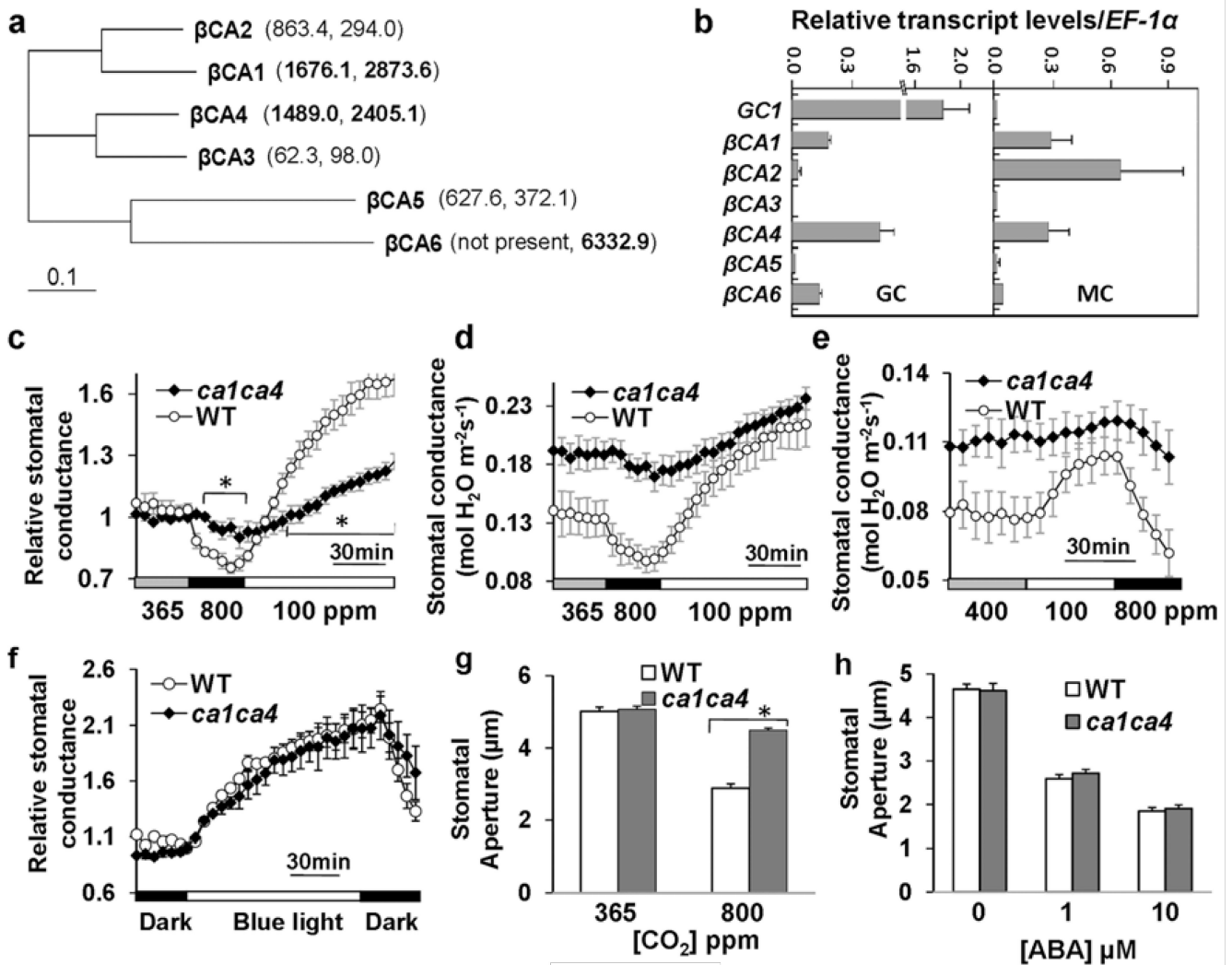


Figure 1. Disruption of the carbonic anhydrases β CA1 and β CA4 greatly impairs CO₂-induced stomatal movements, but not responses to blue light and abscisic acid

(a) Phylogenetic tree (ClustalX 1.83) of *Arabidopsis* β -carbonic anhydrases (β CAs) and corresponding average guard cell specific microarray expression data in brackets (Left, 8K AG Genechips21; Right, ATH1 Genechips22). β CA1, β CA4 and β CA6 showed the highest expression values among β CAs within guard cells as depicted in bold. β CA1 (At3g01500), β CA2 (At5g14740), β CA3 (At1g23730), β CA4 (At1g70410), β CA5 (At4g33580) and β CA6 (At1g58180)²⁴. (b) Relative transcript levels (compared to *EF-1 α* , At5g60390) of the six β CA genes in guard cells (GC) and mesophyll cells (MC) (qRT-PCR, $n = 3$ independent biological replicates, \pm s.e.m.). qRT-PCR data confirmed high expression of β CA1, β CA4 and β CA6 in guard cells. *GCI*, At1g22690²². (c–e) Time-resolved stomatal conductance responses to [CO₂] concentrations in wild-type (WT) and *calca4* mutant plants (c, d, $n = 7$; e, $n = 5$ leaves). (c) shows normalized responses of those shown in d. * means significant difference in the bracketed points between *calca4* and wild-type plants ($P < 0.05$, unpaired Students *t*-test). For initial rates of stomatal conductance changes in d: for 800 ppm to 100 ppm shift, dConductance/dt = 0.028 ± 0.005 in wild type and 0.008 ± 0.002 in *calca4*; in e: for 100 ppm to 800 ppm shift, dConductance/dt = -0.034 ± 0.004 in wild type and -0.005 ± 0.009 in *calca4*, mmol H₂O m⁻²s⁻¹, means \pm s.e.m., $P < 0.05$, unpaired *t*-test. (f) Analyses of relative stomatal conductance responses to blue light and light-dark transitions in wild-

type (WT) and *calca4* mutant plants ($n = 4, \pm$ s.e.m.). **(g)** High [CO₂]-induced stomatal closing is impaired in *calca4* mutant leaf epidermes ($n = 4$ experiments, 80 stomata per condition), in which only guard cells and leaf pavement cells were alive and no mesophyll cells were in the vicinity. Leaf epidermes were treated with 800 ppm CO₂ for 30 min. Data represent means \pm s.e.m.. (genotype blind analyses). * $P < 0.001$, pairwise Student's *t*-test. See also Supplementary Information Fig. S2d for a 60 min treatment. **(h)** Stomata in *calca4* leaves close in response to abscisic acid ($n = 3$ experiments, 30 stomata per experiment and condition). Data represent means \pm s.e.m..

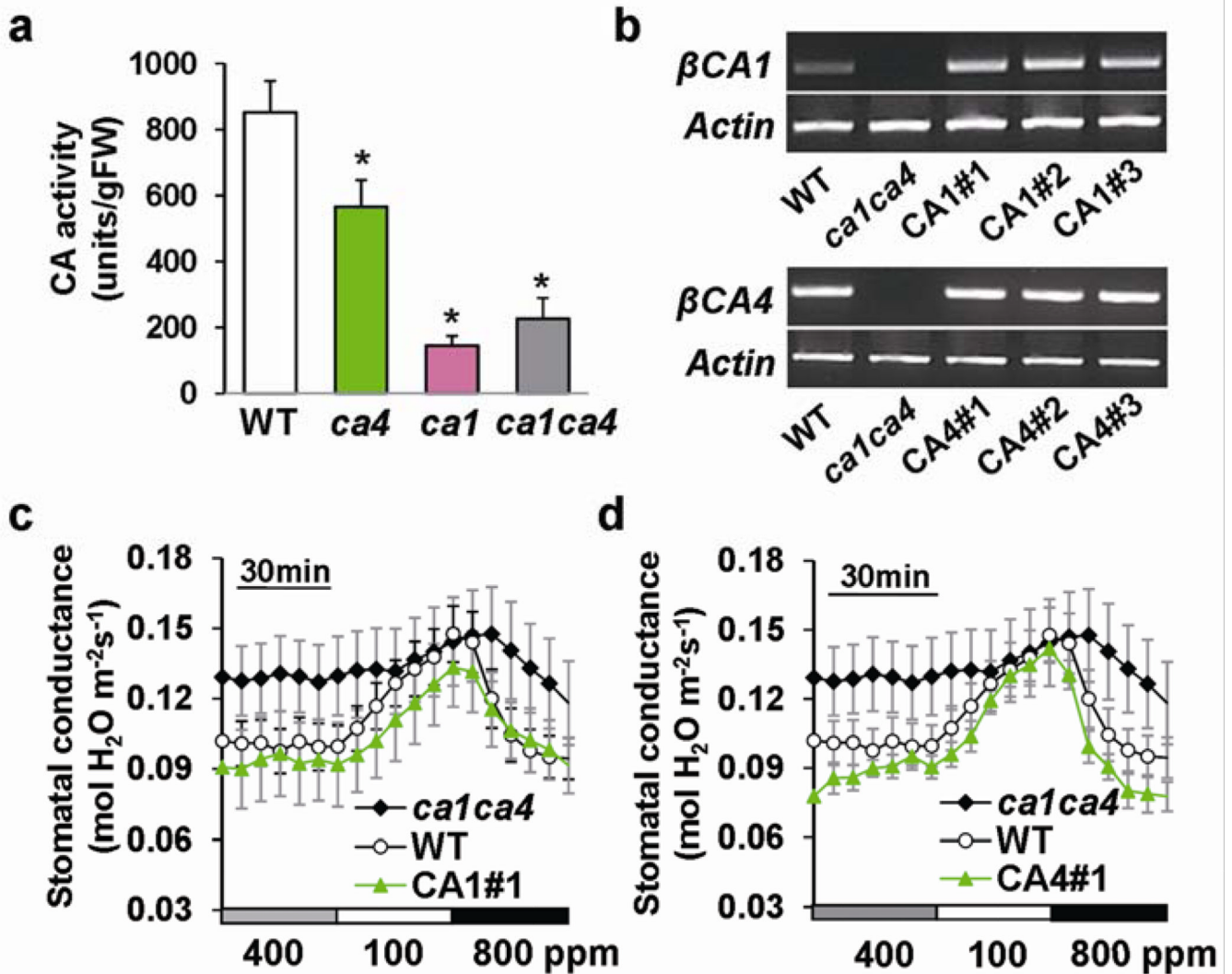


Figure 2. Introduction of wild-type genomic β CA complements the reduced CO₂ sensitivity of *calca4*

(a) Catalytic carbonic anhydrase activity assays show a reduction by 65% in carbonic anhydrase activity of the *calca4* double mutant ($n = 16$) compared to wild-type plants ($n = 16$). Means \pm s.e.m., * $P < 0.05$ compared to wild type, unpaired Student's *t*-test. Residual carbonic anhydrase activities were not significantly different between *ca1* and *calca4* mutant plants ($P > 0.3$, pairwise Student's *t*-test). (b) RT-PCR analyses confirmed restoration of β CA1 and β CA4 expression in *calca4* leaves transformed with genomic β CA1 or β CA4 constructs. Three independent randomly selected transgenic lines per genomic construct were analyzed. *Actin* (At2g37620) was used as a control. (c) Complementation line with genomic β CA1 construct exhibits recovery of [CO₂]-regulated stomatal conductance changes ($n = 8$ leaves for *calca4*, $n = 10$ for WT and $n = 4$ for each complemented line). Means \pm s.e.m.. (d) Complementation line with genomic β CA4 construct exhibits recovery of [CO₂]-regulated stomatal conductance changes ($n = 8$ leaves for *calca4*, $n = 10$ for WT and $n = 4$ for each complemented line). Experiments in c and d were performed in the same experimental set with the same controls. Means \pm s.e.m.. Supplementary Information Fig. S3 shows four other independent transgenic lines analyzed in parallel.

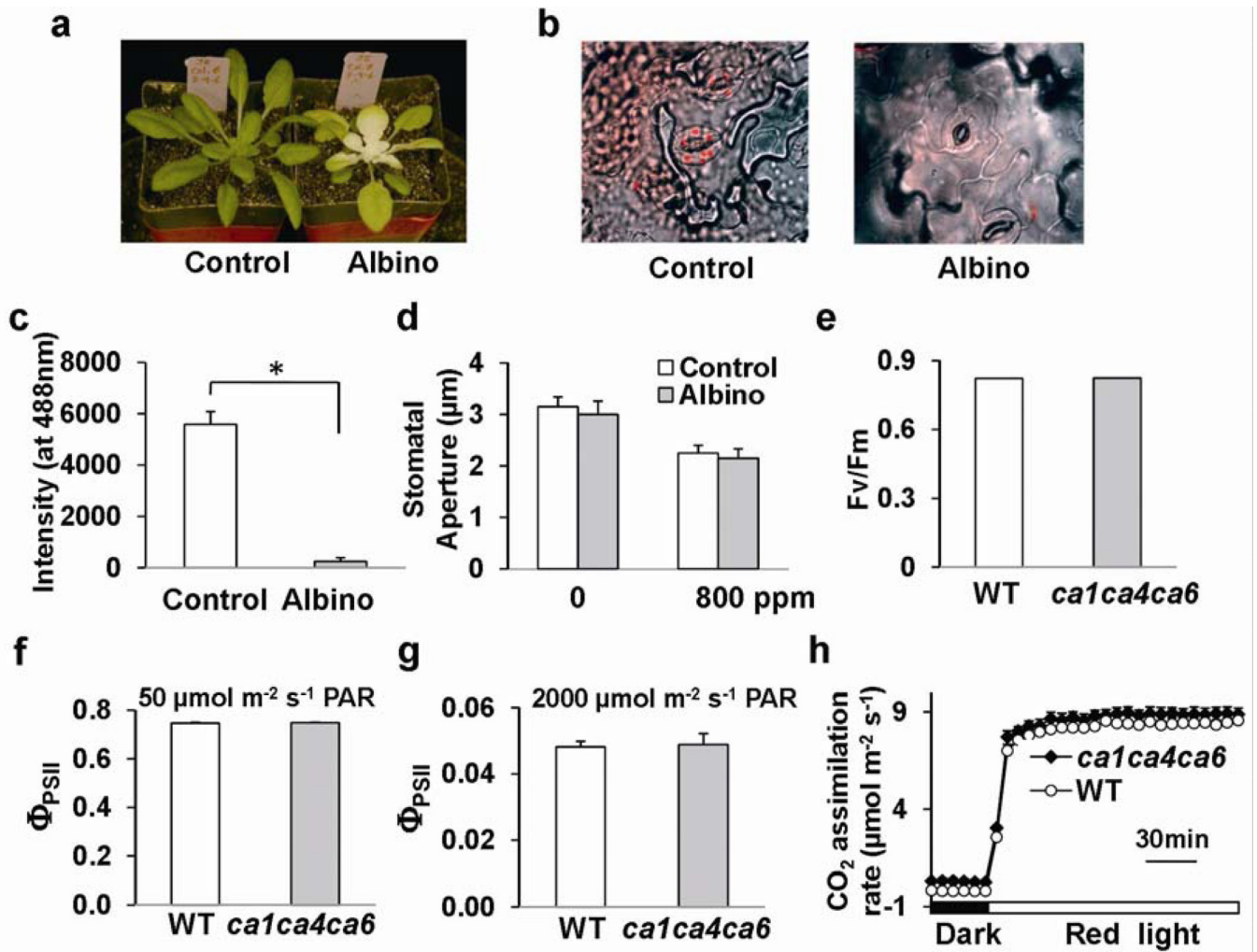


Figure 3. Photosynthesis is not directly linked to β CA-mediated CO₂-triggered stomatal responses

(a) Chlorophyll-deficient albino wild-type leaves were generated by watering with the carotenoid biosynthesis inhibitor norflurazon. (b) Chlorophyll-deficiency in norflurazon-treated albino leaf guard cells compared to wild type was analyzed using confocal microscopy. (c) The absence of chlorophyll in albino guard cells was quantified by image analyses of chlorophyll fluorescence intensity ($n = 3$, 12 stomata/sample). * $P < 0.001$, pairwise Student's t -test. (d) The stomatal CO₂ response to [CO₂] changes was functional in intact albino leaf epidermes ($n = 7$ experiments, 50 stomata/sample). Means \pm s.e.m.. (e) The maximum efficiency of photosystem II (PSII)- F_v/F_m in dark-adapted leaves was unaffected in *ca1ca4ca6* mutant plants ($n = 10$, \pm s.e.m.). (f, g) No difference was observed between wild type (WT) and *ca1ca4ca6* mutant plants with respect to the quantum yield of PSII (Φ_{PSII}) in leaves pre-adapted (f) at $50 \mu\text{mol m}^{-2}\text{s}^{-1}$ ($n = 6$) or (g) at $2000 \mu\text{mol m}^{-2}\text{s}^{-1}$ ($n = 6$) photosynthetically active radiation. Means \pm s.e.m. (h) Red light ($300 \mu\text{mol m}^{-2}\text{s}^{-1}$) - induced CO₂ assimilation of intact leaves was not impaired in *ca1ca4ca6* plants ($n = 6$, \pm s.e.m.).

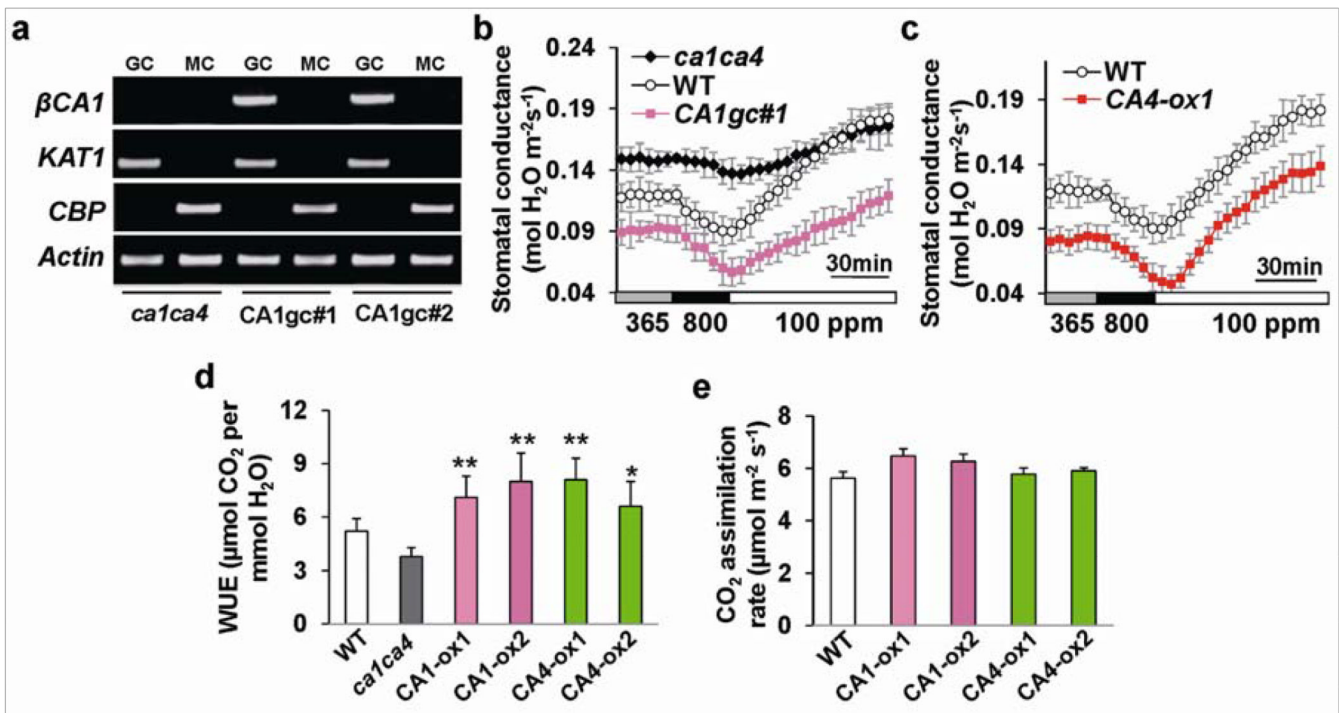


Figure 4. βCA expression in *ca1ca4* guard cells restores CO₂ responses and βCA over-expression plants show improved instantaneous water use efficiency

(a) RT-PCR analyses of $\beta CA1$ expression in guard cell (GC) and mesophyll cell (MC) protoplasts of two *ca1ca4* lines expressing $\beta CA1$ driven by the *pGCI* promoter. GC, guard cell; MC, mesophyll cell. *KAT1*, At5g46240, leaf guard cell marker; *CBP*, At4g33050, mesophyll cell marker. (b) $\beta CA1$ expression in guard cells restores CO₂ responsiveness in intact leaves. CO₂-induced stomatal conductance changes of guard cell-targeted line CA1gc#1 and *ca1ca4* and wild-type plants from the same experimental set ($n = 4$). Fig. S7 shows CO₂ responses of other independent transgenic lines. Note that the starting stomatal conductance in guard cell-targeted lines was lower than that in wild type, probably because *pGCI* drives stronger expression in guard cells²² than the native βCA promoters (Fig. 1b). (c) Stomatal conductance of $\beta CA4$ over-expressing lines and wild-type (WT) plants in response to the indicated [CO₂] changes ($n = 4$, \pm s.e.m.). Fig. S8 shows other independent transgenic lines analyzed in parallel. Experiments in (b) and (c) were performed in the same experimental set with the same controls. (d) $\beta CA1$ and $\beta CA4$ over-expressing lines show improved instantaneous water use efficiency (WUE, $\mu\text{mol CO}_2$ assimilated per mmol H₂O transpired). $n = 5$, error bars depict means \pm s.e.m.. $P < 0.01$ (**) and $P < 0.05$ (*), compared to wild type, pairwise Student's *t*-test. (e) Rates of photosynthesis (CO₂ assimilation) at ambient (365 ppm) [CO₂] in wild type and the analyzed $\beta CA1$ and $\beta CA4$ guard cell over-expressing lines. Error bars depict means \pm s.e.m..

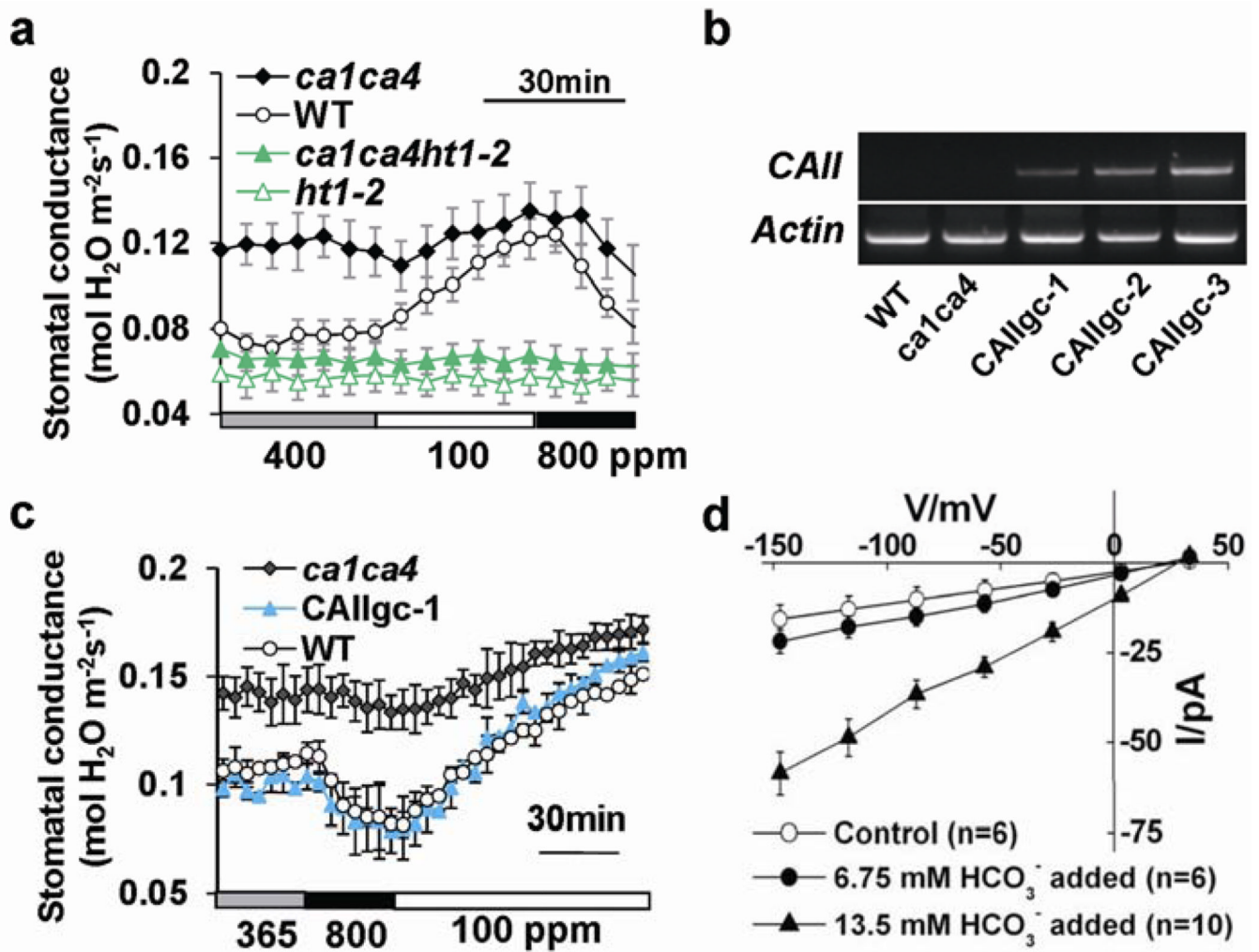


Figure 5. HT1 epistasis analysis, human *aCAII* expression in guard cells restores CO₂ responsiveness and HCO₃⁻ regulation of anion channels

(a) Time-resolved stomatal conductance analyses in *ca1ca4* ($n = 4$), wild-type ($n = 4$), *ht1-2* ($n = 7$) and *ca1ca4ht1-2* triple mutant ($n = 7$) leaves in response to the indicated [CO₂] changes, show that HT1 is epistatic to β CA1 and β CA4. (b) RT-PCR analyses show human *aCAII* expression in randomly selected human *aCAII* transgenic *ca1ca4* plant leaves. (c) Stomatal conductance of guard cell-targeted human *aCAII*-expressing *ca1ca4* lines, *ca1ca4* and wild-type plants in response to the indicated [CO₂] changes ($n = 4$, \pm s.e.m.). Three human *aCAII*-expressing lines were randomly chosen for stomatal response experiments and all showed recovery of CO₂ responsiveness. Fig. S10 shows two other independent transgenic lines analyzed in parallel. (d) Elevated bicarbonate activates S-type anion channel currents in *Arabidopsis* guard cells. Average current-voltage curves were recorded in wild-type guard cells at ambient conditions (open circles) or with intracellular addition of either 13.5 mM bicarbonate, buffered to 2 mM free CO₂ (filled red triangles) or 6.75 mM bicarbonate, buffered to 1 mM free CO₂ (filled circles). Error bars depict means \pm s.e.m..